



A single-point mutation enhances dual functionality of a scorpion toxin



Xueli Wang, Bin Gao, Shunyi Zhu*

Group of Peptide Biology and Evolution, State Key Laboratory of Integrated Management of Pest Insects & Rodents, Institute of Zoology, Chinese Academy of Sciences, 1 Beichen West Road, Chaoyang District, 100101 Beijing, China

ARTICLE INFO

Article history:

Received 18 June 2015

Received in revised form 24 August 2015

Accepted 1 September 2015

Available online 7 September 2015

Keywords:

MeuTXK α 3

K⁺ channel toxin

Antibacterial peptide

Mesobuthus eupeus

Scorpion venom

ABSTRACT

Scorpion venom represents a tremendous, hitherto partially explored peptide library that has been proven to be useful not only for understanding ion channels but also for drug design. MeuTXK α 3 is a functionally unknown scorpion toxin-like peptide. Here we describe new transcripts of this gene arising from alternative polyadenylation and its biological function as well as a mutant with a single-point substitution at site 30. Native-like MeuTXK α 3 and its mutant were produced in *Escherichia coli* and their toxic function against *Drosophila Shaker* K⁺ channel and its mammalian counterparts (rK_v1.1–rK_v1.3) were assayed by two-electrode voltage clamp technique. The results show that MeuTXK α 3 is a weak toxin with a wide-spectrum of activity on both *Drosophila* and mammalian K⁺ channels. The substitution of a proline at site 30 by an asparagine, an evolutionarily conserved functional residue in the scorpion α -KTx family, led to an increased activity on rK_v1.2 and rK_v1.3 but a decreased activity on the *Shaker* channel without changing the potency on rK_v1.1, suggesting a key role of this site in species selectivity of scorpion toxins. MeuTXK α 3 was also active on a variety of bacteria with lethal concentrations ranging from 4.66 to 52.01 μ M and the mutant even had stronger activity on some of these bacterial species. To the best of our knowledge, this is the first report on a bi-functional short-chain peptide in the lesser Asian scorpion venom. Further extensive mutations of MeuTXK α 3 at site 30 could help improve its K⁺ channel-blocking and antibacterial functions.

© 2015 Elsevier Inc. All rights reserved.

1. Introduction

Scorpion venom is a combinational library of ion channel-targeted neurotoxins, cytolytic peptides, proteinases and inhibitors, antimicrobial peptides, and other toxic components (Diaz et al., 2009; Ma et al., 2012; Abdel-Rahman et al., 2013; Cao et al., 2013; He et al., 2013; Mille et al., 2014), and its essential biological function is involved in capturing prey (e.g. insects) and defending against predators (e.g. birds, lizards, and mammals) (Polis, 1990; Inceoglu et al., 2003). Peptide neurotoxins are a major component of scorpion venom, most of which impair functions of Na⁺ and K⁺ channels. Scorpion toxins affecting K⁺ channels (abbreviated as KTxs) typically contain 23–64 amino acids with three or four disulfide bridges. They fold into a typical cysteine-stabilized α/β scaffold (CS $\alpha\beta$) shared with insect and fungal defensins (Quintero-Hernández et al., 2013; Zhu et al., 2014). According to sequence similarity and disulfide pattern, these molecules can be grouped into four large families: α -, β -, γ -, and κ -KTxs (Quintero-Hernández et al., 2013). The α -KTx family, usually containing 23–42 amino acids with 3 or 4 disulfide bridges (Tytgat et al., 1999; Quintero-Hernández et al., 2013), is the most diverse scorpion toxin group among those affecting voltage-gated K⁺ channels (K_v), which in turn reflects their

targets' diversity. These molecules have been proven to be useful tools for studying pharmacological, physiological, and structural characteristics of different subtypes of K⁺ channels (Wickenden, 2002; López-González et al., 2003; Rodríguez de la Vega et al., 2003).

MeuTXK α 3 is a functionally unknown scorpion toxin-like peptide of 38 residues, belonging to the α -KTx family. It was identified by screening a venom gland cDNA library from *Mesobuthus eupeus* (Zhu et al., 2011). Despite low sequence similarity to other known KTxs, this peptide contains typical structural residues (six cysteines and one glycine in the GKC motif) involved in the formation of a CS $\alpha\beta$ folding and a functional dyad (Lys27 and Phe36) for K⁺ channel blockade. In this work, we describe for the first time the bi-functional feature of MeuTXK α 3 as a K⁺ channel toxin with antibacterial activity, and guided by prior knowledge, we designed a mutant to improve its dual functions.

2. Materials and methods

2.1. cDNA cloning

Reverse-transcriptional PCR was used to isolate new transcripts encoding MeuTXK α 3 via two rounds of amplifications with nested PCR primers (MeuTxK α 3-F0 and MeuTxK α 3-F1) (Table 1). Nucleotide sequences reported here have been deposited in GenBank (<http://www>.

* Corresponding author. Tel.: +86 10 64807112; fax: +86 10 64807099.

E-mail address: Zhusy@ioz.ac.cn (S. Zhu).

URL: <http://english.ipm.ioz.cas.cn/re/group/zhushunyi/> (S. Zhu).

Table 1

Primers used in this study.

Name	Sequence	Usage
MeuTxK α 3-F0	5'-ATAATTATAACGAGATATAGACA-3'	Gene isolation
MeuTxK α 3-F1	5'-CGCTTTCCATTGTTCTACAATTA-3'	Gene isolation
MeuTxK α 3-FP	5'-GGATCCGATGACGATGACAAGGTA GATTTTCCTAATAAAA-3'	Construction of expression vector
MeuTxK α 3-RP	5'-GTCGACTTATCCTGGAAAACATCT GCA-3'	Construction of expression vector
MeuTxK α 3-30FP	5'- AATA ATTATTGCAGATGTTTCCA GGA-3'	Mutation
MeuTxK α 3-30RP	5'-AAAGCATTTCCTCTGTAATTAAG-3'	Mutation

Note: Mutated nucleotides are boldfaced. All primers listed here were synthesized by SBS Genetech (Beijing, China).

ncbi.nlm.nih.gov/) under accession numbers of EF442052, EF442053, KR493338–KR493340.

2.2. Sequence and structure analysis

Sequences used in this study were retrieved from GenBank and were aligned by CLUSTAL (<http://www.ebi.ac.uk/Tools/msa/clustalw2/>). The model structure of P30N was built according to the previously described method for MeuTxK α 3 (Zhu et al., 2011). The NMR structure of ChTX (PDB entry 2CRD), a well-characterized scorpion α -KTx, was used as template for comparative modeling on SWISS-MODEL, a fully automated protein structure homology-modeling server (<http://swissmodel.expasy.org>) and models were evaluated by the Verify 3D (Eisenberg et al., 1997).

2.3. Construction of recombinant expression vectors

To construct pGEX-4 T-1-MeuTxK α 3 expression vector, we amplified the MeuTxK α 3 cDNA using primers MeuTxK α 3-FP and MeuTxK α 3-RP (Table 1) by standard PCR, as described previously (Yuan et al., 2007). We introduced a *Bam* HI site and codons of the enterokinase (EK) cleavage site (DDDDK) at the 5' end of the FP and a *Sal* I site and a stop codon at the 5' end of the RP. PCR product was firstly cloned into pGM-T and sequenced by T7 primer. Recombinant plasmid confirmed was digested by *Bam* HI and *Sal* I and then ligated into pGEX-4 T-1.

2.4. Site-directed mutagenesis

Inverse PCR, as previously described (Zhu et al., 2008; Wang et al., 2015), was used to generate the mutant P30N. Phosphorylation of the 5'-end of primers (Table 1) was performed with polynucleotide kinase and ATP. PCR products were circularized by T4 DNA ligase and transformed into *E. coli* DH5 α competent cells. Positive clones were confirmed by DNA sequencing.

2.5. Expression, purification, and characterization of recombinant peptides

Expression of glutathione-S-transferase-MeuTxK α 3 and P30N in *E. coli* Rosetta (DE3) was induced by 0.5 mM IPTG. Fusion proteins were obtained from the supernatant after sonication, followed by affinity chromatography with glutathione-Sepharose 4B beads from GE Healthcare (Shanghai, China). The fusion proteins in 1 \times PBS buffer (140 mM NaCl, 2.7 mM KCl, 10 mM Na₂HPO₄, and 1.8 mM KH₂PO₄, pH7.3) were then digested with EK (Sinobio Biotech Co. Ltd., Shanghai, China) at 25 $^{\circ}$ C overnight. RP-HPLC was applied to separate MeuTxK α 3 and P30N from the enzymatic product. Molecular masses of recombinant peptides were determined by MALDI-TOF mass spectra.

2.6. Circular dichroism spectroscopy

CD spectra of MeuTxK α 3 and P30N were recorded on ChirascanTM-plus circular dichroism spectrometer (Applied Photophysics Ltd, United Kingdom), which were measured at room temperature from 190 to 260 nm with a quartz cell of 1.0 mm thickness. Data were collected at 1 nm intervals with a scan rate of 60 nm/min. Percentages of peptide secondary structure elements were calculated with the DICHROWEB software, an online server for protein secondary structure analysis from CD data (<http://dichroweb.cryst.bbk.ac.uk>).

2.7. Expression of K⁺ channels in *Xenopus* oocytes

For the expression of K_v channels (rK_v1.1–rK_v1.3 and *Shaker* IR) in *Xenopus* oocytes, linearized plasmids were transcribed with the T7 mMMESSAGE-mMACHINE transcription kit (Ambion, USA) (Gao et al., 2010). Oocytes were obtained from anesthetized female *Xenopus laevis*, as described previously (Liman et al., 1992). The oocytes were digested for 1–2 h by treatment with 0.5 mg/ml collagenase I at room temperature in Ca²⁺ free ND96 solution, and then washed 3 times with Ca²⁺-free ND96 and another 3 times with ND96 (96 mM NaCl, 2 mM KCl, 1.8 mM CaCl₂, 2 mM MgCl₂, and 5 mM HEPES, pH7.4 with NaOH). Oocytes of stage V–VI were selected and cultured in ND96 containing 50 mg/l gentamycin sulfate at 18 $^{\circ}$ C. After 2–3 h incubation, oocytes were injected with cRNA by micro-injector (NANOLITER 2000, WPI) and then incubated in ND96 solution with 50 mg/l gentamycin sulfate at 18 $^{\circ}$ C for 1–5 days.

2.8. Electrophysiological recording

Two-electrode voltage-clamp recordings were performed at room temperature with an Oocyte Clamp Amplifier (OC-725C, Harvard Apparatus Company) controlled by a data acquisition system (Digidata 1440A, Axon CNS) dominated by pCLAMP10.2 software (Axon Inc., USA). Whole-cell currents from oocytes were recorded 2–5 days after injection. Bath solution was ND96 solution. Voltage and current electrodes were pulled by P-97 Flaming/Brown Micropipette Puller (Sutter Instrument Co., USA) with resistance of 0.1–1.0 M Ω when filled with 3 M KCl. The elicited currents were filtered at 1 kHz and sampled at 2 kHz by a four-pole low pass Bessel filter. Leak subtraction was performed with a P/4 protocol. Currents were evoked by 250 ms depolarizations to 0 mV followed by a 250 ms pulse to –50 mV, from a holding potential of –90 mV. Data were analyzed by pClamp Clampfit 10.0 (Molecular Devices) and SigmaPlot 11.0 (Systat Software, CA, USA).

2.9. Antibacterial assays

Antibacterial assays were carried out according to the literature (Hultmark, 1998). *Bacteria* were incubated at 37 $^{\circ}$ C in Broth medium until the OD₆₀₀ reached 0.6. 10 μ l of bacterial culture was mixed in 6 ml of Broth medium containing 0.8% agar and poured into Petri dishes of 9.0 cm diameter. Wells with a diameter of 2 mm were punched into the medium, filled with 2 μ l of sample each well. *Bacteria* were incubated at 37 $^{\circ}$ C for 12 h and then zone of inhibition was measured. Lethal concentration (C_L) was calculated according to the Hultmark method

Table 2

Comparison of lethal concentration (C_L) of MeuTxK α 3 and P30N on different bacterial species.

Bacteria	MeuTxK α 3	P30N	Fold
<i>Bacillus megaterium</i> CGMCC 1.0459	14.26	4.95	2.9
<i>Bacillus subtilis</i> CGMCC 1.2428	10.28	6.11	1.7
<i>Micrococcus luteus</i> CGMCC 1.0290	4.66	5.50	0.9
<i>Streptococcus mutans</i>	33.80	24.06	1.4
<i>Xanthomonas oryzae</i>	52.01	17.68	2.9

Note: Concentrations are given in μ M and fold is calculated as C_L of the wild peptide/C_L of the mutant.

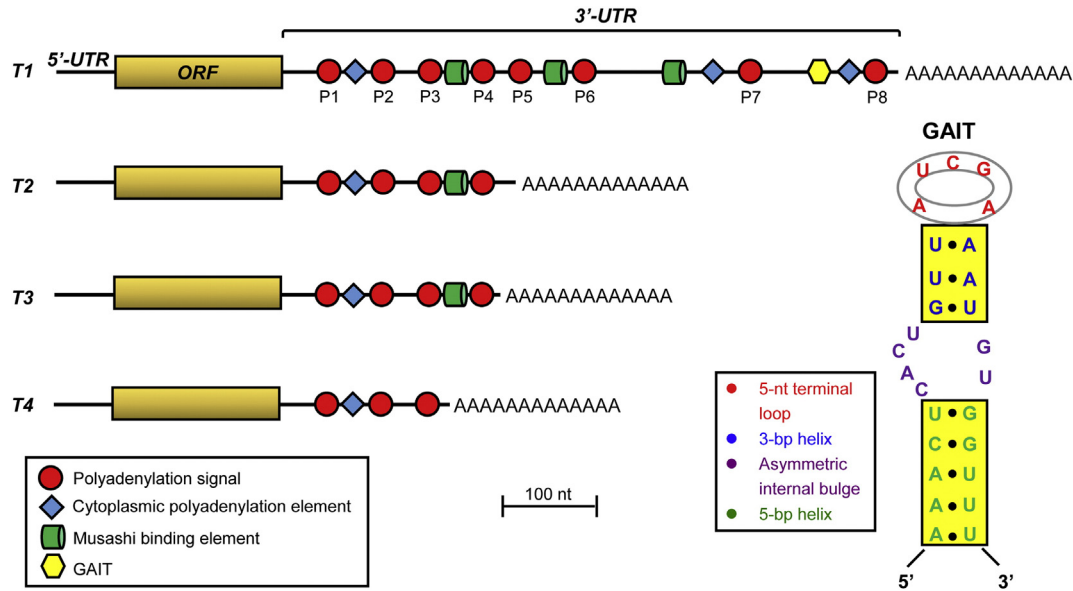


Fig. 1. 3'-UTR analysis. Schematic diagrams of 3'-UTRs of MeuTXKα3 with multiple functional motifs indicated. T1–T4 represent transcript 1 to transcript 4, with different sizes in their 3'-UTRs due to alternative usage of poly(A) signals. The GAIT motif was recognized by RegRNA (<http://regrna2.mbc.nctu.edu.tw/>).

(Hultmark, 1998). Bacterial species used in this study were listed in Table 2.

2.10. Membrane permeability assays

To assess the permeation ability of MeuTXKα3 and P30N on bacterial membrane, 5×10^5 *B. megaterium* cells in 500 μL of PBS were mixed with 1 μM propidium iodide for 5 min in dark (Zhu et al., 2012). After peptide was added, the increase in fluorescence, owing to the binding of the dye to intracellular DNA, was measured with a F-4500 FL spectrophotometer (Hitachi High-Technology Company). Once basal fluorescence reaches a constant value, peptide (MeuTXKα3, P30N or muccin-18) or vancomycin was added. Changes in fluorescence arbitrary were monitored ($\lambda_{exc} = 525$ nm; $\lambda_{ems} = 595$ nm) and plotted as arbitrary units.

3. Results and discussion

3.1. New transcripts of MeuTXKα3 arising from alternative polyadenylation

In this work, we isolated several new transcripts of MeuTXKα3 by nested RT-PCR, which contain different 3'-UTRs in size, ranging from 166 to 663 bp (Fig. 1). Sequence analysis combined with motif recognition revealed multiple functional motifs in MeuTXKα3 involved in mRNA processing and translational regulation: 1) A total of eight poly(A) signals (P1–P8) with a consensus hexamer (AAUAAA, UAUAAA, and AUUAAA) were characterized in the longest transcript (T1), in which P3, P4, and P8 act as signals to generate all the transcripts described here, T1–T4 (Fig. 1); 2) Three cytoplasmic polyadenylation elements (CPEs) (UUUUAAU) were recognized, each of which is located upstream of a poly(A) signal, with a distance to a poly(A) signal 4–

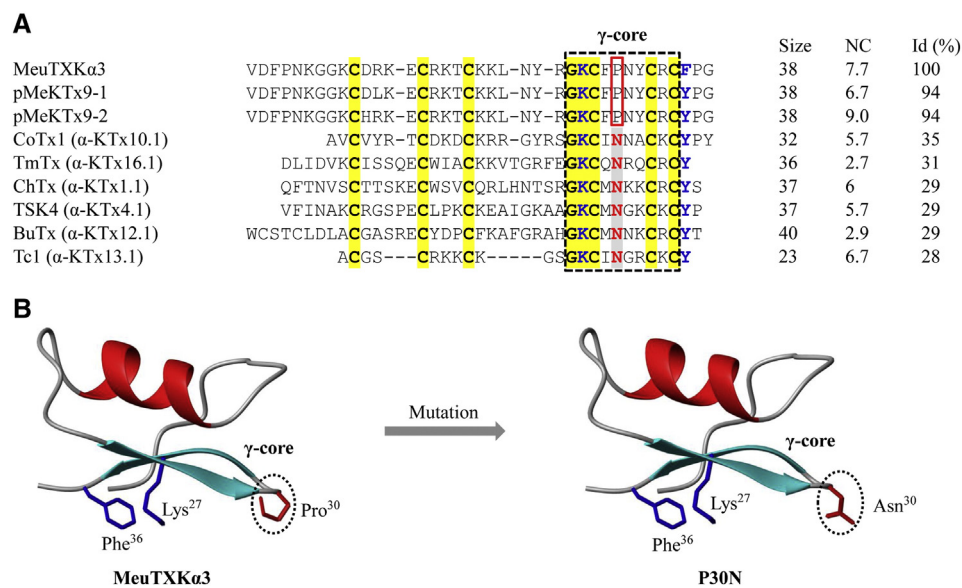


Fig. 2. Sequence and structure of features of MeuTXKα3. (A) Multiple sequence alignment of MeuTXKα3 with other scorpion toxins. Identical residues are shadowed in yellow. Evolutionarily conserved Lys and Asn residues are shown in color and the structurally equivalent residue of the Asn in the three toxins (Pro) is boxed. The γ -core region is boxed in dotted line format. Sequence sources (Gimenez-Gallego et al., 1988; Rogowski et al., 1994; Escoubas et al., 1997; Selisko et al., 1998; Batista et al., 2000; Holaday et al., 2000); (B) The ribbon diagrams of MeuTXKα3 and P30N with structure and functional elements highlighted.

76 nt (Fig. 1). It is found that this element can direct either inhibition or activation of target mRNA translation via its binding protein, CPEB, depending on the cellular context (Richter, 2007); 3) Three Musashi binding elements (MBEs) are scattered in the 3'-UTR (Fig. 1). It has been shown that efficient translation of DNMT1, a DNA (cytosine-5)-methyltransferase, requires both CPE and MBE elements (Rutledge et al., 2014); 4) An IFN-gamma-activated inhibitor of translation (GAIT) element specifically exists in the longest 3'-UTR, which displays a typical GAIT signature, composed of a 5-nt terminal loop, a weak 3-bp helix, an asymmetric internal bulge, and a proximal 5-bp helix. It is known that GAIT is sufficient for translational silencing both *in vitro* and *in vivo* in human (Sampath et al., 2003). The specific presence of a GAIT in the longest transcript and other functional motifs with different numbers suggest that each mRNAs described here may possess differential translational efficiency to regulate the expression of this

gene and thus could provide an explanation for the alternative polyadenylation of *MeuTXK α 3*.

It is also worth mentioning that alternative polyadenylation also occurs in two other scorpion toxin genes (*BmTXK β 2* and *Opiscorpine*) (Zhu et al., 1999; Zhu and Tytgat, 2004). These observations might be helpful in further investigation of alternative tailing-mediated regulation mechanism of scorpion venom gland-expressed genes.

3.2. Sequence and structure characteristics of *MeuTXK α 3*

As shown in Fig. 2A, *MeuTXK α 3* displays the highest similarity to two functionally unknown toxin-like peptides from the same scorpion species (pMeKTx9-1 and pMeKTx9-2) (Kuzmenkov et al., 2015), but only 28%–35% similarity to other α -KTxs previously identified (Zhu et al., 2011) (Fig. 2A). It has been found that this peptide contains a

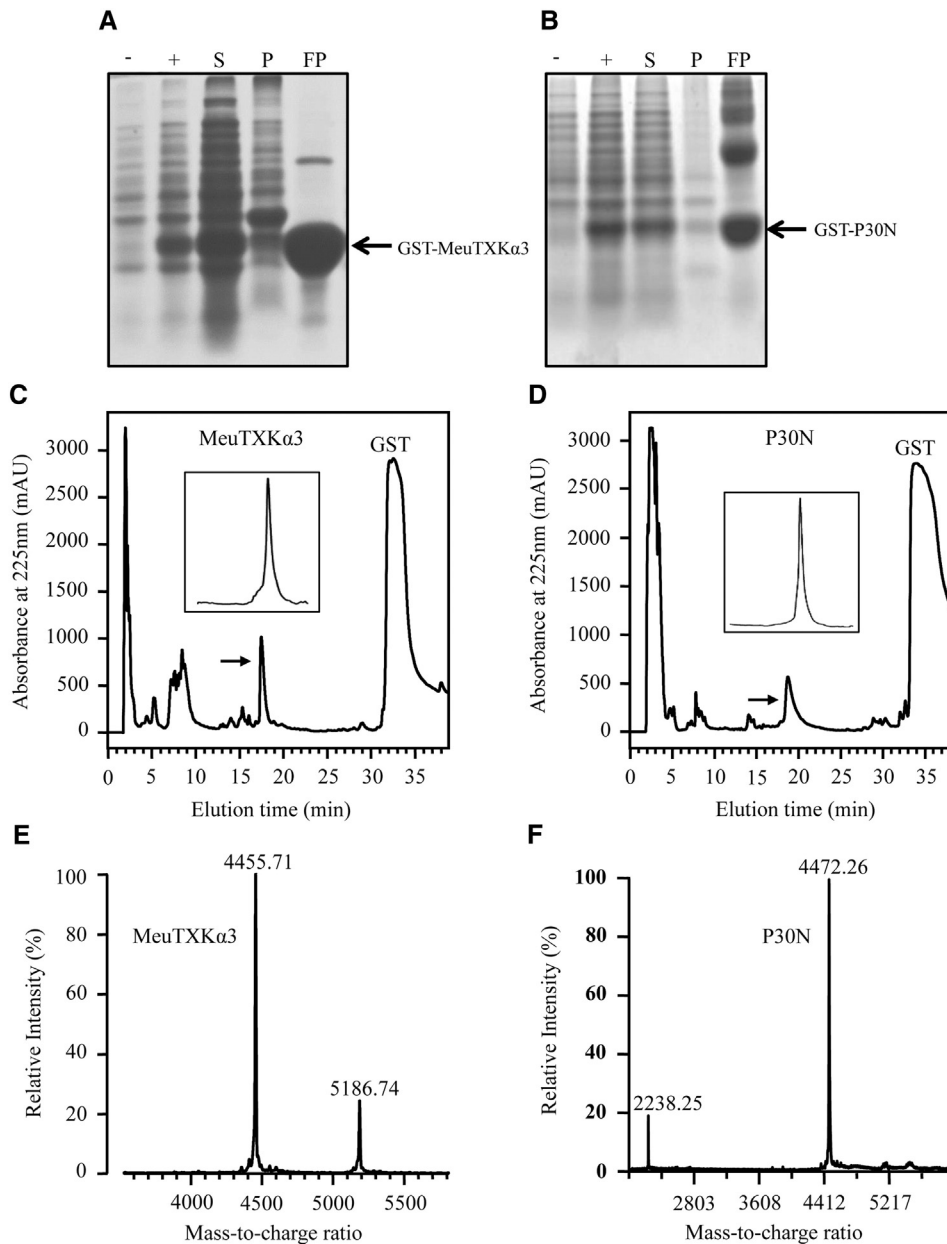


Fig. 3. Expression, purification, and characterization of peptides. (A, B) SDS-PAGE showing the expression and purification of *MeuTXK α 3* (A) and P30N (B). -: total cell extract of *E. coli* carrying pGEX-4 T-1-*MeuTXK α 3* and pGEX-4 T-1-P30N without IPTG; +: IPTG-induced total cell extract; S and P: supernatant and pellet, respectively, from the cell lysate prepared by sonication; FP: the eluted fusion protein from glutathione-Sepharose 4B resin. Fusion proteins are labeled by arrows; (C, D) RP-HPLC showing the purified *MeuTXK α 3* and P30N. C_{18} column was equilibrated with 0.1% TFA in water (v/v) and the purified proteins were eluted from the column with a linear gradient from 0% to 60% acetonitrile in 0.1% TFA within 40 min. Inset, repurification of recombinant peptides; (E, F) MALDI-TOF determining molecular masses of *MeuTXK α 3*, and P30N.

putative functional dyad (Lys27 and Phe36) involved in interacting with the pore of K⁺ channels (Zhu et al., 2011); however, a crucial Asn at site 30 located in a four-residue long motif around the fourth cysteine (Lys-Cys-Xaa-Asn, Xaa, any amino acid) of the α -KTx family is substituted by a Pro in MeuTXK α 3 and its two closely related peptides (Fig. 2A). This Asn belongs to the scorpion toxin signature (STS) due to its evolutionary conservation and direct interaction with the pore helix of K_v channels (Lange et al., 2006; Zhu et al., 2014). In view of its functional importance, we designed a mutant of MeuTXK α 3 at site 30 from Pro to Asn (denoted as P30N) expectantly to improve the activity of this naturally occurring peptide. Fig. 2B shows structural models of MeuTXK α 3 and its mutant with positions of the dyad and the mutated amino acid emphasized (Fig. 2B).

3.3. Recombinant MeuTXK α 3 and P30N adopt similar structures

Both MeuTXK α 3 and P30N were expressed in *E. coli* as soluble GST fusion proteins (Fig. 3A and B) that were subjected to EK digestion and subsequent RP-HPLC isolation, from which we collected their products corresponding to retention times of 17.5 and 18.6 min, respectively (Fig. 3C and D). Their molecular masses were confirmed by MALDI-TOF that gave rise to 4455.71 Da for MeuTXK α 3 and 4472.26 Da for P30N (Fig. 3E and F), both well matching their theoretical values 4455.26 and 4472.24 Da, respectively.

Circular dichroism (CD) was used to compare the structures of MeuTXK α 3 and P30N. Overall, the mutation led to no significant structural impact on the peptide, as identified by their similar CD spectra: a minimum at 208 nm and a maximum at 195–198 nm (Fig. 4A), in consistent with MMTX, a scorpion venom-derived K_v channel toxin whose CS α β fold has been confirmed by NMR experiments (Wang et al., 2015). Estimation of percentages of secondary structural elements in these peptides from their CD data revealed that MeuTXK α 3 and P30N had similar turn and unordered contents (Fig. 4B). In comparison with MMTX, MeuTXK α 3 and P30N had a higher β -sheet content (30% vs 18%) but a lower α -helix content (42% vs 53%). This could reflect their sequence difference, sharing only 28% similarity.

3.4. Dual functionality of MeuTXK α 3 enhanced by a single-point mutation

We evaluated the effect of MeuTXK α 3 on four K_v channels (rK_v1.1, rK_v1.2, rK_v1.3, and *Shaker* IR) expressed in *Xenopus* oocytes. The results showed that it exhibited a weak but wide-spectrum blocking activity on all the channels tested here (Fig. 5A). In comparison with the unmodified peptide, the mutation from Pro to Asn at site 30 significantly improves its activity on rK_v1.2 and rK_v1.3 but leads to no influence on the activity of rK_v1.1 and a reduced activity on the *Drosophila Shaker* channel (Fig. 5B and C).

In view of the presence of a γ -core structural motif, an extensively distributed functional domain in a diversity of antimicrobial folds (Yount and Yeaman, 2004), in their C-terminus halves (Fig. 2B), we thus tested antibacterial activity of MeuTXK α 3 and P30N against five species of bacteria (Table 2). The results showed that MeuTXK α 3 inhibited the growth of these bacteria in a concentration-dependent manner (Fig. 5D), with lethal concentrations ranging from 4.66 to 52.01 μ M. The mutation (P30N) significantly improved the antibacterial activity of this peptide on some species. For example, the potency of the mutant on *Bacillus megaterium* and *Xanthomonas oryzae* increased approximately twofolds relative to the unmodified peptide. (Table 2). Action mode studies showed that these two peptides were capable of causing membrane damage slowly and slightly (Fig. 5E), as assessed by the fluorescent nucleic acid-binding dye propidium iodide. This is in contrast to meucin-18, a melittin-like cytolytic peptide from scorpion venom (Gao et al., 2009), which causes an immediate fluorescent increase upon exposure of the peptide (Fig. 5E). A slow curve indicates that the membrane disruption evoked by MeuTXK α 3 and P30N is a gradual process. Similar case was also observed in several plant

defensins (Van der Weerden et al., 2010). Relative to MeuTXK α 3, P30N had a slightly stronger membrane-damaged capability, which might partly account for its more potent activity (Fig. 5E).

Taken together, our results demonstrate that MeuTXK α 3 is a dually functional molecule as a K⁺ channel blocker and antibacterial peptide, whose activity is enhanced by site 30 in the γ -core (Fig. 2B). The functional importance of this site could be associated with its structural location on a loop linking two β -strands. Firstly, in terms of the K⁺ channel toxicity, differential selectivity for the mammalian channel subtypes was observed between this peptide and its mutant. This might be a reflection of different residues on the interacting face of these channels with the toxins. According to our and others' established toxin-channel interaction, site 30 is a functional site of α -KTxs for binding to the channel turret region and pore helix (Banerjee et al., 2013; Zhu et al., 2014). Given nearly identical sequences in the pore helix between *Shaker* and the three mammalian K⁺ channels, we suspected that the turret region with remarkable amino acid difference is key determinants for distinguishing differential sensitivity of the channels to the two toxins. Although the activity of P30N on the two mammalian channels increased, its decrease on *Shaker* suggests that evolutionary fixation of a Pro in this toxin is favorable for its insect toxicity. Secondly, regarding the antibacterial activity of MeuTXK α 3, site 30 is situated in a functional γ -core domain of many antimicrobial defensins (Gao and Zhu, 2010). It is possible that substitution in this functional domain enhanced the activity of this peptide through introducing a more hydrophilic Asn facilitating the formation of a local amphipathic structure.

3.5. Possible biological function of MeuTXK α 3

Some other dually functional peptides were also characterized previously in scorpion venoms. For example, MeuTXK β 1, a scorpion venom-derived two-domain K_v channel toxin-like peptide with neurotoxic and cytolytic activities (Zhu et al., 2010); Hg1, a member of the scorpion Kunitz-type K_v channel toxin family specific for K_v1.3 channels (Chen et al., 2012); ChTx, a typical K_v channel blocker with antimicrobial activity (Gimenez-Gallego et al., 1988; Yount and Yeaman, 2004). Apart from scorpion venom, the sea anemone *Anthopleura elegantissima* venom also contains a toxin (APEKTx1) with Kunitz type protease and

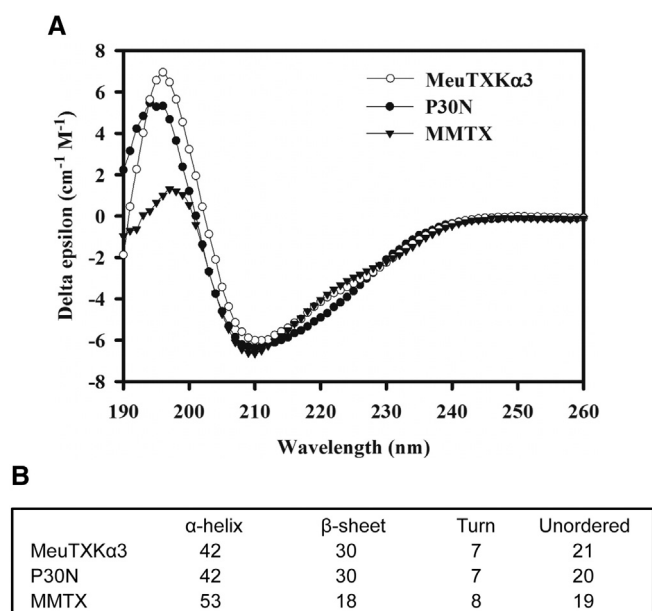


Fig. 4. CD spectra of MeuTXK α 3 and P30N. (A) The spectra were recorded from 190 to 260 nm with a peptide concentration of 0.1 mg/ml in water. MMTX, a newly characterized scorpion toxin specific for K⁺ channels (Wang et al., 2015), was used as control. (B) Comparison of percentages of peptide secondary structure elements from the CD data among MeuTXK α 3, P30N, and MMTX (Wang et al., 2015).

K_v -inhibiting properties (Peigneur et al., 2011). Thus, it is possible that toxins with dual functionality extensively exist in animal venoms, presumably due to their unique functional features involved in both prey on animals and defense against microorganisms.

In spite of weak in vitro activity, there are two lines of evidence in favor of functional importance of MeuTXK α 3: 1) MeuTXK α 3 has multiple transcripts to putatively regulate its translation; 2) Like MeuTXK α 3, scorpion venom contains some other weakly toxic components. For example, members from the κ -KTx and λ -KTx families block K^+ channels at high micromolar concentrations (Srinivasan et al., 2002; Nirthanan et al., 2005; Camargos et al., 2011; Vandendriessche et al., 2012; Gao et al., 2013). The existence of multiple weak components with different molecular folds in scorpion venom supports their non-redundancy. Given the fact that a nontoxic mutant *Bj*-xtrIT-E15R can enhance Lqh α IT binding (Cohen et al., 2006), it is reasonable to infer that MeuTXK α 3

might exert its biological function by synergy with other active venom components to be commonly responsible for scorpion's defense and attack.

4. Conclusions

In this study, we carried out structural and functional characterization of a new scorpion venom-derived dually functional peptide (MeuTXK α 3) and highlighted a key site whose mutation enhanced the dual functionality of this peptide. MeuTXK α 3 folds into an α -KTx structure and functions as inhibitors of both K_v channels and bacteria. Given key role of site 30 in activity, further mutations of this site as well as its neighboring region could help improve its K^+ channel-blocking and antibacterial functions, which would thus provide a

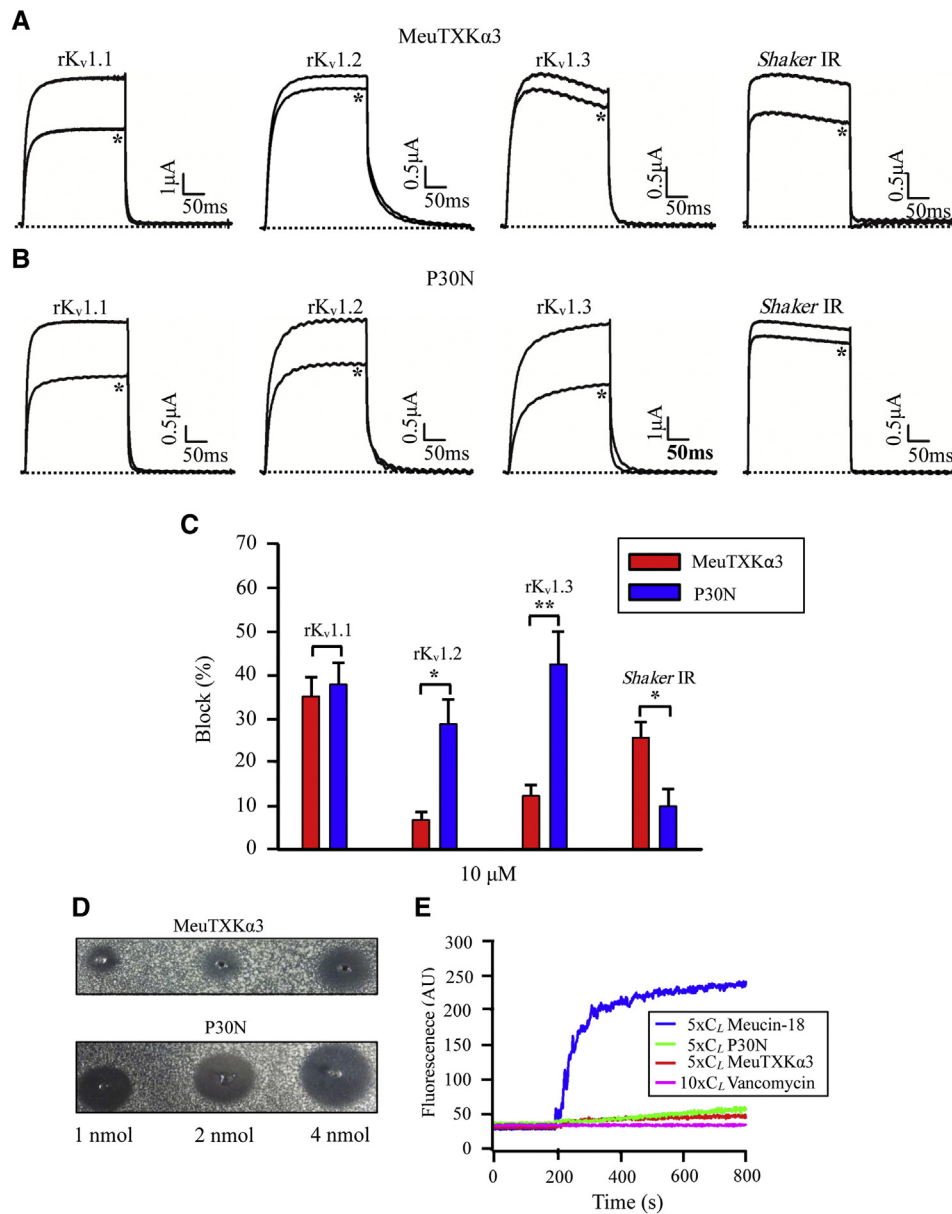


Fig. 5. The P30N mutation affects the dual functionality of MeuTXK α 3. (A, B) MeuTXK α 3 and P30N differentially inhibit different K_v channels expressed in *Xenopus* oocytes. Representative whole-cell current traces are shown. The dotted line indicates the zero-current level. Asterisks mark steady-state current traces after application of 10 μ M peptides. Traces shown are representative traces of at least three independent experiments ($n \geq 3$); (C) Comparison of blocking effect between MeuTXK α 3 and P30N. Data are shown as mean \pm SE ($n \geq 3$) and statistical analysis was performed using one-way ANOVA followed by Student Newman Keuls post hoc test to compare between two peptides with SPSS (SPSS Inc.). * $P < 0.05$; ** $P < 0.01$; (D) Concentration-dependent inhibition of *B. megaterium* by MeuTXK α 3 and P30N; (E) PI experiments evaluated impact of peptides on bacterial membrane integrity. In each run, MeuTXK α 3 or P30N at 5x C_L was added when the basal fluorescence remained constant for 200 s. Vancomycin (Schneider et al., 2010) and meucine-18 (Gao et al., 2009) were used as negative and positive control, respectively.

valuable molecular template and strategy to design peptides with specific and enhanced function.

Acknowledgments

We would like to thank Prof. O. Pongs for providing rK_v1.1, rK_v1.2, and rK_v1.3; Prof. G. Yellen for *Shaker* IR. This work was supported by the National Natural Science Foundation of China (31570773 and 31221091) and the State Key Laboratory of Integrated Management of Pest Insects and Rodents (Grant Nos. ChineseIPM1307, ChineseIPM1405, and ChineseIPM1512).

References

- Abdel-Rahman, M.A., Quintero-Hernandez, V., Possani, L.D., 2013. Venom proteomic and venomous glands transcriptomic analysis of the Egyptian scorpion *Scorpio maurus palmatus* (Arachnida: Scorpionidae). *Toxicon* 74, 193–207.
- Banerjee, A., Lee, A., Campbell, E., Mackinnon, R., 2013. Structure of a pore-blocking toxin in complex with a eukaryotic voltage-dependent K⁺ channel. *Elife* 2, e00594.
- Batista, C.V., Gómez-Lagunas, F., Lucas, S., Possani, L.D., 2000. Tc1, from *Tityus cambridgei*, is the first member of a new subfamily of scorpion toxin that blocks K⁺ channels. *FEBS Lett.* 486, 117–120.
- Camargos, T.S., Restano-Cassulini, R., Possani, L.D., Peigneur, S., Tytgat, J., Schwartz, C.A., Alves, E.M., de Freitas, S.M., Schwartz, E.F., 2011. The new kappa-KTx 2.5 from the scorpion *Opisthacanthus cayaporum*. *Peptides* 32, 1509–1517.
- Cao, Z., Yu, Y., Wu, Y., Hao, P., Di, Z., He, Y., Chen, Z., Yang, W., Shen, Z., He, X., Sheng, J., Xu, X., Pan, B., Feng, J., Yang, X., Hong, W., Zhao, W., Li, Z., Huang, K., Li, T., Kong, Y., Liu, H., Jiang, D., Zhang, B., Hu, J., Hu, Y., Wang, B., Dai, J., Yuan, B., Feng, Y., Huang, W., Xing, X., Zhao, G., Li, X., Li, Y., Li, W., 2013. The genome of *Mesobuthus martensii* reveals a unique adaptation model of arthropods. *Nat. Commun.* 4, 2602.
- Chen, Z.Y., Hu, Y.T., Yang, W.S., He, Y.W., Feng, J., Wang, B., Zhao, R.M., Ding, J.P., Cao, Z.J., Li, W.X., Wu, Y.L., 2012. Hg1, novel peptide inhibitor specific for K_v1.3 channels from first scorpion Kunitz-type potassium channel toxin family. *J. Biol. Chem.* 287, 13813–13821.
- Cohen, L., Lipstein, N., Gordon, D., 2006. Allosteric interactions between scorpion toxin receptor sites on voltage-gated Na channels imply a novel role for weakly active components in arthropod venom. *FASEB J.* 20, 1933–1935.
- Diaz, P., D'Suze, G., Salazar, V., Sevcik, C., Shannon, J.D., Sherman, N.E., Fox, J.W., 2009. Antibacterial activity of six novel peptides from *Tityus discrepans* scorpion venom. A fluorescent probe study of microbial membrane Na⁺ permeability changes. *Toxicon* 54, 802–817.
- Eisenberg, D., Lüthy, R., Bowie, J.U., 1997. VERIF3D: assessment of protein models with three-dimensional profiles. *Methods Enzymol.* 277, 396–404.
- Escoubas, P., Romi-Lebrun, R., Lebrun, B., Herrmann, R., Moskowitz, H., Rajendra, W., Hammock, B., Nakajima, T., 1997. Tamulotoxin, a novel member of the potassium channel active short toxins from the venom of the Indian red scorpion *Buthus tamulus*. *Toxicon* 35 (806–806).
- Gao, B., Zhu, S., 2010. Identification and characterization of the parasitic wasp *Nasonia deficiens*: positive selection targeting the functional region? *Dev. Comp. Immunol.* 34, 659–668.
- Gao, B., Sherman, P., Luo, L., Bowie, J., Zhu, S., 2009. Structural and functional characterization of two genetically related meucien peptides highlights evolutionary divergence and convergence in antimicrobial peptides. *FASEB J.* 23, 1230–1245.
- Gao, B., Peigneur, S., Tytgat, J., Zhu, S., 2010. A potent potassium channel blocker from *Mesobuthus eupeus* scorpion venom. *Biochimie* 92, 1847–1853.
- Gao, B., Harvey, P.J., Craik, D.J., Ronjat, M., De Waard, M., Zhu, S., 2013. Functional evolution of scorpion venom peptides with an inhibitor cysteine knot fold. *Biochem. Biophys. Res. Commun.* 433, 3–8.
- Gimenez-Gallego, G., Navia, M.A., Reuben, J.P., Katz, G.M., Kaczorowski, G.J., Garcia, M.L., 1988. Purification, sequence, and model structure of charybdotoxin, a potent selective inhibitor of calcium-activated potassium channels. *Proc. Natl. Acad. Sci. U. S. A.* 85, 3329–3333.
- He, Y., Zhao, R., Di, Z., Li, Z., Xu, X., Hong, W., Wu, Y., Zhao, H., Li, W., Cao, Z., 2013. Molecular diversity of Chaerilidae venom peptides reveals the dynamic evolution of scorpion venom components from Buthidae to non-Buthidae. *J. Proteome* 89, 1–14.
- Holaday Jr., S.K., Martin, B.M., Fletcher Jr., P.L., Krishna, N.R., 2000. NMR solution structure of butantoxin. *Arch. Biochem. Biophys.* 379, 18–27.
- Hultmark, D., 1998. Quantification of antimicrobial activity, using the inhibition zone assay. In: Dumphy, A.G., Marmaras, V.J. (Eds.), *Techniques in Insect Immunology*. Lavoisier Press, FL, pp. 103–107.
- Inceoglu, B., Lango, J., Jing, J., Chen, L., Doymaz, F., Pessah, I.N., Hammock, B.D., 2003. One scorpion, two venoms: pre-venom of *Parabuthus transvaalicus* acts as an alternative type of venom with distinct mechanism of action. *Proc. Natl. Acad. Sci. U. S. A.* 100, 922–927.
- Kuzmenkov, A.I., Vassilevski, A.A., Kudryashova, K.S., Nekrasova, O.V., Peigneur, S., Tytgat, J., Feofanov, A.V., Kirpichnikov, M.P., Grishin, E.V., 2015. Variability of potassium channel blockers in *Mesobuthus eupeus* scorpion venom with focus on Kv1.1: AN INTEGRATED TRANSCRIPTOMIC AND PROTEOMIC STUDY. *J. Biol. Chem.* 29, 12195–12209.
- Lange, A., Giller, K., Hornig, S., Martin-Eauclaire, M.F., Pongs, O., Becker, S., Baldus, M., 2006. Toxin-induced conformational changes in a potassium channel revealed by solid-state NMR. *Nature* 440, 959–962.
- Liman, E.R., Tytgat, J., Hess, P., 1992. Subunit stoichiometry of a mammalian K⁺ channel determined by construction of multimeric cDNAs. *Neuron* 9, 861–871.
- López-González, I., Olamendi-Portugal, T., De la Vega-Beltrán, J.L., Van der Walt, J., Dyason, K., Possani, L.D., Felix, R., Darszon, A., 2003. Scorpion toxins that block T-type Ca²⁺ channels in spermatogenic cells inhibit the sperm acrosome reaction. *Biochem. Biophys. Res. Commun.* 300, 408–414.
- Ma, Y., He, Y., Zhao, R., Wu, Y., Li, W., Cao, Z., 2012. Extreme diversity of scorpion venom peptides and proteins revealed by transcriptomic analysis: Implication for proteome evolution of scorpion venom arsenal. *J. Proteome* 75, 1563–1576.
- Mille, B.G., Peigneur, S., Diego-García, E., Predel, R., Tytgat, J., 2014. Partial transcriptomic profiling of toxins from the venom gland of the scorpion *Parabuthus stridulus*. *Toxicon* 83, 75–83.
- Nirthanan, S., Pil, J., Abdel-Mottaleb, Y., Sugahara, Y., Gopalakrishnakone, P., Joseph, J.S., Sato, K., Tytgat, J., 2005. Assignment of voltage-gated potassium channel blocking activity to kappa-KTx1.3, a non-toxic homologue of kappa-hefutoxin-1, from *Heterometrus spinifer* venom. *Biochem. Pharmacol.* 69, 669–678.
- Peigneur, S., Billen, B., Derua, R., Waelkens, E., Debaveye, S., Béress, L., Tytgat, J., 2011. A bifunctional anemone peptide with Kunitz type protease and potassium channel inhibiting properties. *Biochem. Pharmacol.* 82, 81–90.
- Polis, G.A., 1990. *The Biology of Scorpions*. Stanford University Press, Stanford, CA.
- Quintero-Hernández, V., Jiménez-Vargas, J.M., Gurrola, G.B., Valdivia, H.H., Possani, L.D., 2013. Scorpion venom components that affect ion-channels function. *Toxicon* 76, 328–342.
- Richter, J.D., 2007. CPEB: a life in translation. *Trends Biochem. Sci.* 32, 279–285.
- Rodríguez de la Vega, R.C., Merino, E., Becerril, B., Possani, L.D., 2003. Novel interactions between K⁺ channels and scorpion toxins. *Trends Pharmacol. Sci.* 24, 222–227.
- Rogowski, R.S., Krueger, B.K., Collins, J.H., Blaustein, M.P., 1994. Tityustoxin K alpha blocks voltage-gated noninactivating K⁺ channels and unblocks inactivating K⁺ channels blocked by alpha-dendrotoxin in synaptosomes. *Proc. Natl. Acad. Sci. U. S. A.* 91, 1475–1479.
- Rutledge, C.E., Lau, H.T., Mangan, H., Hardy, L.L., Sunnotel, O., Guo, F., MacNicol, A.M., Walsh, C.P., Lees-Murdock, D.J., 2014. Efficient translation of Dnmt1 requires cytoplasmic polyadenylation and Musashi binding elements. *PLoS One* 9, e88385.
- Sampath, P., Mazumder, B., Seshadri, V., Fox, P.L., 2003. Transcript-selective translational silencing by gamma interferon is directed by a novel structural element in the ceruloplasmin mRNA 3' untranslated region. *Mol. Cell. Biol.* 23, 1509–1519.
- Schneider, T., Kruse, T., Wimmer, R., Wiedemann, I., Sass, V., Pag, U., Jansen, A., Nielsen, A.K., Mygind, P.H., Raventós, D.S., Neve, S., Ravn, B., Bonvin, A.M., De Maria, L., Andersen, A.S., Gammelgaard, L.K., Sahl, H.G., Kristensen, H.H., 2010. Plectasin, a fungal defensin, targets the bacterial cell wall precursor Lipid II. *Science* 328, 1168–1172.
- Selisko, B., Garcia, C., Becerril, B., Gómez-Lagunas, F., Garay, C., Possani, L.D., 1998. Cobatoxins 1 and 2 from *Centruroides noxius* Hoffmann constitute a subfamily of potassium-channel-blocking scorpion toxins. *Eur. J. Biochem.* 254, 468–479.
- Srinivasan, K.N., Sivaraja, V., Huys, I., Sasaki, T., Cheng, B., Kumar, T.K., Sato, K., Tytgat, J., Yu, C., San, B.C., Ranganathan, S., Bowie, H.J., Kini, R.M., Gopalakrishnakone, P., 2002. κ-Hefutoxin1, a novel toxin from the scorpion *Heterometrus fulvipes* with unique structure and function. Importance of the functional diad in potassium channel selectivity. *J. Biol. Chem.* 277, 30040–30047.
- Tytgat, J., Chandy, K.G., Garcia, M.L., Gutman, G.A., Martin-Eauclaire, M.F., van der Walt, J.J., Possani, L.D., 1999. A unified nomenclature for short-chain peptides isolated from scorpion venoms: α-KTx molecular subfamilies. *Trends Pharmacol. Sci.* 20, 444–447.
- Van der Weerden, N.L., Hancock, R.E., Anderson, M.A., 2010. Permeabilization of fungal hyphae by the plant defensin NaD1 occurs through a cell wall-dependent process. *J. Biol. Chem.* 285, 37513–37520.
- Vandendriessche, T., Kopljar, I., Jenkins, D.P., Diego-García, E., Abdel-Mottaleb, Y., Vermassen, E., Clynen, E., Schoofs, L., Wulff, H., Snyders, D., Tytgat, J., 2012. Purification, molecular cloning and functional characterization of HelaTx1 (*Heterometrus laoticus*): the first member of a new κ-KTx subfamily. *Biochem. Pharmacol.* 83, 1307–1317.
- Wang, X., Umetsu, Y., Gao, B., Ohki, S., Zhu, S., 2015. Mesomartoxin, a new K_v1.2-selective scorpion toxin interacting with the channel selectivity filter. *Biochem. Pharmacol.* 93, 232–239.
- Wickenden, A., 2002. K⁺ channels as therapeutic drug targets. *Pharmacol. Ther.* 94, 157–182.
- Yount, N.Y., Yeaman, M.R., 2004. Multidimensional signatures in antimicrobial peptides. *Proc. Natl. Acad. Sci. U. S. A.* 101, 7363–7368.
- Yuan, Y., Gao, B., Zhu, S., 2007. Functional expression of a *Drosophila* antifungal peptide in *Escherichia coli*. *Protein Expr. Purif.* 52, 457–462.
- Zhu, S., Tytgat, J., 2004. The scorpine family of defensins: gene structure, alternative polyadenylation and fold recognition. *Cell. Mol. Life Sci.* 61, 1751–1763.
- Zhu, S., Li, W., Zeng, X., Jiang, D., Mao, X., Liu, H., 1999. Molecular cloning and sequencing of two 'short chain' and two 'long chain' K⁺ channel-blocking peptides from the Chinese scorpion *Buthus martensii* Karsch. *FEBS Lett.* 457, 509–514.
- Zhu, S., Wei, L., Yamasaki, K., Gallo, R.L., 2008. Activation of cathepsin L by the cathelin-like domain of protegrin-3. *Mol. Immunol.* 45, 2531–2536.
- Zhu, S., Gao, B., Aumelas, A., del Carmen Rodríguez, M., Lanz-Mendoza, H., Peigneur, S., Diego-García, E., Martin-Eauclaire, M.F., Tytgat, J., Possani, L.D., 2010. MeuTXβ1, a scorpion venom-derived two-domain potassium channel toxin-like peptide with cytotoxic activity. *Biochim. Biophys. Acta* 1804, 872–883.
- Zhu, S., Peigneur, S., Gao, B., Luo, L., Jin, D., Zhao, Y., Tytgat, J., 2011. Molecular diversity and functional evolution of scorpion potassium channel toxins. *Mol. Cell. Proteomics* 10, M110.002832.
- Zhu, S., Gao, B., Harvey, P.J., Craik, D.J., 2012. Dermatophytic defensin with anti-infective potential. *Proc. Natl. Acad. Sci. U. S. A.* 109, 8495–8500.
- Zhu, S., Peigneur, S., Gao, B., Umetsu, Y., Ohki, S., Tytgat, J., 2014. Experimental conversion of a defensin into a neurotoxin: implications for origin of toxic function. *Mol. Biol. Evol.* 31, 546–559.